REPORT DOCUMENTATION PAGE

Form Approved
OMB No. 0704-0188

1. REPORT DATE *(DD-MM-YYYY)*	**2. REPORT TYPE**	**3. DATES COVERED** *(From - To)*
10-Dec-2003	Technical Paper	

4. TITLE AND SUBTITLE

Plume Interactions of Multiple Jets Expanding into Vacuum

5a. CONTRACT NUMBER

5b. GRANT NUMBER

5c. PROGRAM ELEMENT NUMBER

6. AUTHOR(S)

S. Gimelshein, A. Alexeenko, N. Selden (Univ of So. Calif); A. Ketsdever (AFRL/RZSA); M. Ivanov (Inst. Of Theoretical and Applied Mechanics, Novosibirsk, Russia)

5d. PROJECT NUMBER

5e. TASK NUMBER

5f. WORK UNIT NUMBER
2308M19B

7. PERFORMING ORGANIZATION NAME(S) AND ADDRESS(ES)

AFRL/RZSA
10 E. Saturn Blvd.
Edwards AFB CA 93524-7048

8. PERFORMING ORGANIZATION REPORT NUMBER

9. SPONSORING / MONITORING AGENCY NAME(S) AND ADDRESS(ES)

Air Force Research Laboratory (AFMC)
AFRL/RZS
5 Pollux Drive
Edwards AFB CA 93524-7048

10. SPONSOR/MONITOR'S ACRONYM(S)

11. SPONSOR/MONITOR'S NUMBER(S)
AFRL-PR-ED-TP-2003-321

12. DISTRIBUTION / AVAILABILITY STATEMENT

Approved for Public Release; distribution Unlimited.

13. SUPPLEMENTARY NOTES

 Published by the American Institute of Aeronautics and Astronautics, Inc. AIAA paper no. AIAA-2004-1348.

14. ABSTRACT

Numerical and experimental results for a rarefied gas expansion through a thin circular orifice are presented. The orifice flow was used as a calibration test for a torsional thrust stand designated to measure force levels from 10^{-6} to 10^{-3} N. Molecular nitrogen, argon, and helium at room temperature are used as test gasees. The mass flux and thrust measurements are compared with the direct simulation Monte Carlo results for Knudsen numbers from 40 to 0.01 and plenum to facility background pressure ratios of 10^{3} –10^{7}. Factors that affect the total propulsive force, such as jet backflow and facility background gas penetrating the jet, are analyzed. The measured and calculated mass flux and total propulsive force were found to agree well for Knudsen numbers less than 1.

15. SUBJECT TERMS

16. SECURITY CLASSIFICATION OF:			**17. LIMITATION OF ABSTRACT**	**18. NUMBER OF PAGES**	**19a. NAME OF RESPONSIBLE PERSON**
					Andrew Ketsdever
a. REPORT	**b. ABSTRACT**	**c. THIS PAGE**	SAR	10	**19b. TELEPHONE NUMBER** *(include area code)*
Unclassified	**Unclassified**	**Unclassified**			N/A

Standard Form 298 (Rev. 8-98)
Prescribed by ANSI Std. 239.18

42nd AIAA Aerospace Sciences Meeting and Exhibit
5 - 8 January 2004, Reno, Nevada

AIAA 2004-1348

Plume Interactions of Multiple Jets Expanding into Vacuum: Experimental and Numerical Investigation

A. Ketsdever
Air Force Research Laboratory, Edwards AFB, CA
N. Selden, S. Gimelshein, and A. Alexeenko
University of Southern California, Los Angeles, CA
P. Vashchenkov and M. Ivanov
Institute of Theoretical &.Applied Mechanics, Novosibirsk, Russia

Abstract

The main objective of this work is to examine the impact of jet interactions in arrays of micropropulsion devices on thrust performance. Rarefied flow of nitrogen and helium from a single orifice and orifice arrays into vacuum was studied experimentally and numerically. The chamber pressure was changed in the range from 10 milli-torr to 40 torr, the orifice diameter was 1 mm, and the center-to-center distance between orifices varied from 1.5 to 4 orifice diameters. The direct simulation Monte Carlo (DSMC) method was used in all computations. Good agreement between the experimental and numerical mass flow and thrust values was observed. A large impact of gas back flow was predicted numerically for an infinite array of orifices, that resulted in a specific impulse increase of up to 20 percent.

1 Introduction

The interactions of multiple propulsive plumes expanding into vacuum are becoming increasingly important with the development of microspacecraft. Many micropropulsion system concepts involve the use of thruster arrays operating simultaneously for orbital maneuvers such as attitude control and orbit raising [1, 2]. Arrays of thrusters make operational sense for microspacecraft since thrusters can be conveniently batch fabricated into arrays using Microelectromechanical Systems (MEMS) techniques. The thruster array allows for increased flexibility for microspacecraft since thrusters can be fired in specific sequences or simultaneously to vary the impulse profile and thrust level as desired for a particular maneuver.

The collisional interaction of multiple thruster plumes can have several effects on spacecraft operations such as changes in overall thruster performance, increased heat flux to critical surfaces, and contamination. For example, molecular collisions in the plume interaction region beyond the thruster array exit plane can increase the number of molecules that populate thruster backflow regions (i.e. high angles relative to the thrust direction), which can make the contamination of payloads and sensors more likely. Backscattered molecules can also lead to relatively high heat flux to spacecraft surfaces leading to thermal control issues.

This study is intended to investigate the plume interactions of simultaneously operating free jets expanding into vacuum. Underexpanded orifices are used to simulate gas driven micropropulsion systems. Both experimental and numerical investigation is conducted to compare the performance of a single orifice and that of multiple orifice arrays. Experimental studies are carried out for two test gases, helium and nitrogen, in the range of stagnation pressures from about 10 milli-torr to 40 torr, and included a single and a dual orifice configurations. Numerical studies are performed with the direct simulation Monte Carlo (DSMC) method for nitrogen flow in one-, two-, and four-orifice configurations, as well as in an infinite array of orifices.

2 Experimental setup

All thrust measurements were performed on the nano-Newton Thrust Stand (nNTS) which has been described in detail by Jamison, et. al. [3] The nNTS was installed in Chamber IV of the Collaborative High Altitude Flow Facilities (CHAFF-IV) which is a 3 m diameter by 6 m long cylindrical, high vacuum chamber. The facility was pumped with a 1 m diameter diffusion pump with a pumping speed of 42,000 L/s for helium and 25,000 L/s for molecular nitrogen. The ultimate facility pressure

was approximately 10^{-6} torr with all operational pressures below 10^{-4} torr. A previous study [4] has shown that at these background pressures and corresponding thrust levels, there is no evidence of background pressure effects on the thrust measurements in CHAFF-IV.

The geometry for the single orifice used in this study is shown schematically in Fig. 1. For the single orifice configuration, the orifice is located on the plenum's horizontal and vertical centerlines. The orifice is attached to a plenum with a cross-sectional area much larger than the orifice area to help ensure uniform flow. The orifice diameter is 1.0 mm. The orifice is machined in a 0.5 mm thick aluminum plate giving $t/d = 0.5$. For the dual orifice configuration, the center of the orifices was located 0.75 mm from the plenum's horizontal centerline and aligned along the plenum's vertical centerline. This configuration located both orifices at the same radial distance from the thrust stand center of rotation.

The stagnation pressure in the orifice plenum was measured using calibrated pressure transducers. The propellant is introduced to the plenum through an adjustable needle valve located downstream of a mass flow meter. In the experimental configuration, the mass flow meters were operated in the continuum regime throughout the pressure range investigated. The propellants used were molecular nitrogen and helium. In the configuration used for this study, the stagnation pressures ranged from several milli-Torr to approximately 40 torr for both propellants, and the stagnation temperature was measured to be 295 K throughout this investigation.

The nNTS was calibrated using an electrostatic force calibration technique [5]. The calibration of the force balance deflection uses the verified analytical solution of the electrostatic comb actuator's produced force as a function of the applied potential difference between the comb sections. A unique feature of the nNTS is its ability to measure the force levels of the 1.0 mm orifice from the free molecule through continuum flow ranges. The low thrust measuring capability of the nNTS allows for the investigation of the transitional flow regime.

3 Numerical approach

Gas expansion into vacuum trough thin orifices is associated with strong thermal nonequilibrium in the expansion region. Therefore, a microscopic, kinetic approach has to be used to accurately model such flows numerically. The DSMC method was applied in this work to compute both two- and three-dimensional orifice flows and jet interactions. The DSMC-based software system SMILE [6] was used. The important features of SMILE that are relevant to this work are parallel capability, different collision and macroparameter grids with manual and automatic adaptations, and spatial weighting for axisymmetric flows.

The majorant frequency scheme [7] was used to calculate intermolecular interactions. The intermolecular potential was assumed to be a variable hard sphere [8]. Energy redistribution between the rotational and translational modes was performed in accordance with the Larsen-Borgnakke model. A temperature-dependent rotational relaxation number was used. The reflection of molecules on the surface was assumed to be diffuse with complete energy and momentum accommodation.

The DSMC method is conventionally used to model supersonic and hypersonic flows, where the boundary conditions are either supersonic inflow or vacuum outflow, and their implementation is straightforward. For subsonic flows, such as the flow inside the stagnation chamber, the application of the DSMC method is complicated by the uncertainty in the boundary conditions. Disturbances arising downstream propagate upstream, thus changing the conditions at the inflow boundary. In this case, one of the possible solutions of the problem is to perform calculations in a large domain, so that disturbances propagating upstream would decay due to the viscosity impact before they reach the inflow boundary. A sufficiently small time step has also to be used in order to satisfy one of the principal requirements of the DSMC method (a particle should not cross more than one cell per time step). Zero flow velocity was assumed at the inflow boundaries, with the number flux and temperature corresponding to given stagnation conditions.

To avoid errors related to subsonic boundary conditions, axisymmetric computations were performed first for a single orifice and large computational domain to determine the region where the upstream disturbances are significant. Then, the computations in smaller domains were conducted using axisymmetric and 3D codes, with domain boundaries chosen using the information from the large-domain computations.

All computations were conducted for an infinitesimally thin orifice with molecular nitrogen as the propellant. Note that this differs from the experimental setup, where the wall has a finite thickness. According to the experimental setup, the orifice diameter was $d = 1$ mm. The first set of calculations was performed for a single orifice and a dual orifice configuration with two distances between orifice centers, $2d$ and $4d$. The chamber pressure varied in these computations from 0.01 torr to 4 torr. In order to examine the impact of multiple jet interaction on the orifice thrust performance, the computations in the second set were performed with a more dense flow of 7.6 torr for four orifice configurations, a single orifice, two orifices, four orifices, and an infinite array of orifices. The distance between the adjacent orifice centers in this set was $1.5d$.

Symmetry planes were used in the three-dimensional calculations to reduce computational costs. The

schematic of the geometry used is shown in Fig. 2 in YZ coordinate plane. YZ plane coincides with the orifice plane at X=0, and X axis coincides with the symmetry line of the flow. Two specular surfaces were used in the first three geometries, and four specular surfaces were taken to simulate the flow in an infinite array of orifices.

4 Results and discussion

4.1 Experimental results for dual orifice geometry

Experimental results have been obtained for a single orifice and a dual orifice configuration with a center-to-center separation distance of 1.5 mm operating on the nNTS. Figures 3 and 4 show the experimental results from the single orifice and dual orifice geometries for helium and nitrogen gas flows respectively. The experimental error bars for all of the data are smaller than the physical size of the data points shown.

The mass flow rates in Figs. 3 and 4 represent flow conditions that range from free molecular to near-continuum flow. As expected, there was no influence of the jet impingement for the dual orifice configuration in the free molecular (collisionless) flow regime. However, some influence might be anticipated as the collisional regime is approached (i.e. at higher stagnation pressures).

Within the experimental error, the slopes of the best linear fits through the single and dual orifice data are the same for helium up through a mass flow rate of 1000 sccm. Similarly, the slopes of the best linear fits through the single and dual orifice data are the same for nitrogen up through a mass flow rate of 400 sccm. The data indicates that the influence of the dual jet impingement on the measured performance over the range of stagnation pressures (mass flow rates) investigated in this study is less than the standard deviation of the measured data (1.5%).

4.2 Comparison of measured and computed orifice thrust

A DSMC modeling of three-dimensional flows with subsonic boundary conditions is a numerically challenging task, and obtained results need to be verified. The verification in this work was performed through a comparison of results obtained using the 3D code for a single orifice with the corresponding axisymmetric results and available experimental data [9]. The computations were performed for a molecular nitrogen as the test gas. Figure 5 shows the mass flow rate as a function of gas pressure in the chamber. Note a good agreement between the two sets of numerical results (three-dimensional and axisymmetric) and the measurements. Figure 6 shows a good agreement between the numerical and experimental values of orifice thrust in the entire region of chamber pressures under consideration.

Let us now consider the impact of the distance between the orifice centers on orifice performance for the dual orifice configuration. The results of DSMC calculations are presented in Table 1 for two distances, $S = 2$mm and $S = 4$mm, where they are also compared with the mass flow and thrust values for a single orifice obtained with axisymmetric and three-dimensional codes. Note that for the dual orifice configuration the results are normalized to one orifice to simplify comparison with the single orifice cases. The difference between the mass flow and the thrust for a single orifice and the corresponding values for dual orifice cases is less than 3% for the two distances between the orifice centers. The difference does not allow us to conclude that there is any significant orifice interference, and can rather be attributed to the impact of the boundary conditions and higher level of statistical scatter in three-dimensional calculations.

This conclusion qualitatively agrees with the above conclusion drawn from the present experimental data. The quantitative comparison of numerical and experimental data is given in Fig 7, where the thrust versus mass flow is shown for the single and dual orifice configurations. Again, there is no visible difference between the results for two configurations. The agreement between the numerical results and the measurements is also quite good.

4.3 Multiple jet interactions

Even though both experiments and computations did not show any visible effect of the orifice interference for the dual orifice configuration, such an effect may be significantly larger for an array of orifices. To investigate possible interference, the computations were performed for a four-orifice configuration and a configuration that mimics an infinite array of orifices.

An important part of this study was calculation of the surface force produced by jet molecules. It is clear that the back flow of molecules from the jet creates a force that increases the total thrust generated by orifice. Whereas the backflow from a single orifice is not a significant source of additional thrust, the interaction of multiple jets will certainly amplify the back flow, and therefore increase the corresponding surface force.

The results presented below were obtained with the 3D code for molecular nitrogen and a chamber pressure of 7.6 torr and temperature of 300 K. The distance between adjacent orifice centers was 1.5 mm. The general structure of the flow is given in Fig. 8, where the Mach number fields are shown for four considered configurations. Note that only parts of computational domains are given here in order to provide more detail in the

vicinity of the orifice plane. The top figure illustrates a typical flow pattern for a single orifice (the bottom boundary is the symmetry plane). The upstream influence of the orifice is relatively small (less than the orifice diameter), and the sonic line is located downstream from the orifice plane.

The Mach number field for the dual orifice case is shown in Fig. 8b. Here, the bottom boundary represents the symmetry plane that separates two orifices, and the flow is shown in XY plane that crosses the two orifice centers. It is seen that the interaction between the two orifices is not significant for the upper half of the computational domain. The lower half is affected mostly downstream from the orifice plane. There is a clear interaction between the two orifice jets, and the interaction region at the orifice centerline starts at about one millimeter from the orifice plane.

The flow for the four-orifice configuration is shown in Fig. 8c at XY plane that crosses the centers of two adjacent orifices. The jet interaction is significantly stronger in this case, and ine interference is noticeable both in the lower and upper half of the computational domain. The interaction has also some impact on the subsonic part of the flow.

The last figure shows the Mach number contours for an array of orifices. One orifice of an infinite array is presented here in XY plane. The inflow boundary conditions were different from the other cases, with a finite velocity in X direction of 62 m/s and pressure of 7.44 torr imposed at the inlet. These conditions correspond to the stagnation pressure of 7.6 torr used in the three previous cases. The flow fields for the orifice array configuration are qualitatively different from conventional orifice flow fields. The gas expansion right after the orifice plane is followed by the gas compression due to the jet interaction, and the Mach number decreases in the compression region.

The quantitative impact of orifice jet interactions on gas velocities is shown in Fig. 9, where the flow velocity in X direction is shown along the centerline for the four orifice configurations. There is a small difference between the single and the dual orifice cases. The four orifice case is visibly different starting at about two orifice diameters downstream from the orifice plane. A strong jet interaction in the orifice array causes a large difference both in the upstream and downstream flow regions. The flow reaches its final downstream value at about five orifice diameters. An interesting fact is that the values of flow velocity are almost identical at the orifice plane and in a small vicinity of it for all geometrical conditions.

The jet interference results in higher gas pressure in the interaction region downstream from the orifice, as shown in Fig. 10b. There is a local pressure maximum observed at the symmetry plane about one orifice diameter downstream from the orifice plane. The larger number of orifices (Figs. 10c-d) results in further pressure increase both at the orifice axis and in the back flow region. For the array case, there is a pressure minimum observed at the orifice axis at 2.5 mm from the orifice formed due to the flow expansion immediately after the orifice plane, and a successive compression resulted from the interaction of jets reflected on symmetry planes.

4.4 Multiple orifice performance

The performance of multiple orifices is determined by the thrust force of orifices and the force exerted by the jet backflow on the plenum outer surface. In order to show the impact of the orifice jet interactions on the backflow, a cross section was examined parallel to the orifice plane and located in the cells adjacent to the surface downstream from the orifice. Figure 11 shows the pressure fields at this cross section for different geometries. For a single orifice, the pressure near the most part of the surface is over two orders of magnitude smaller that the chamber pressure, which means that the surface force is expected to be negligible compared to the orifice thrust force. For the dual orifice configuration, the back flow is impacted by the jet interaction only between the orifices. The maximum pressure at the symmetry plane (bottom boundary) for this case amounts to about 2% of the chamber pressure. For the four orifice configuration (symmetry planes are at the left and bottom boundaries), there is a large area where the pressure reaches about 5-7% of the chamber pressure. For the orifice array, the gas pressure near the outer surface ranges from 5 to 10% of the chamber one.

Pressure distribution near the surface for the four geometric conditions extracted along a line is given in Fig. 12. Zero distance from the orifice edge in this figure corresponds to the lowest point of the orifice edge in Fig. 11, and the profiles are extracted along the vertical line coming through this point down to the symmetry plane. In the single orifice case, the pressure decreases quickly with distance, being less than 1% of the chamber pressure of 1,012 Pa. The dual orifice case is characterized by a pressure profile that is essentially flat at about 2.5% of the orifice pressure. The pressure near the surface along the chosen line for the four-orifice flow is also almost constant. In the array case, there is clearly a pressure maximum being formed at the symmetry plane. Note that for the latter two cases, the actual pressure maxima observed on the intersection of diagonal lines coming through centers of opposite orifices are much higher than those shown in Fig. 12.

The performance characteristics of the four considered configurations are listed in Table 2. For all the cases the values are given per one orifice. Since the gas pressure was shown to be significant for multiple jet cases, the surface force F_s is shown separately from

the orifice thrust F_o. The specific impulse is calculated using the total force that consists of F_o and F_s. The axisymmetric single-orifice result is also shown here for comparison. The difference between the mass flow and orifice thrust values for all cases is less than the statistical scatter of the computations (except a somewhat higher orifice thrust for the array case). The conclusion therefore is that there is no significant impact of the jet interference either on the mass flow or thrust.

The force on the surface produced by the gas backflow changes dramatically, though. It increases from about one or two percent of the orifice thrust for a single or dual orifice cases to more than 16% for the orifice array. This is an important result that explains a much higher specific impulse for the array case (the total increase of the specific impulse is over twenty percent compared to the single orifice flow).

5 Conclusions

The primary objective of this work was to study numerically and experimentally the effect of multiple jet interactions on the thrust performance of micropropulsion devices. The interaction between 1 mm orifice jets was studied experimentally for helium and nitrogen and numerically for nitrogen. The stagnation pressure in the experiments ranged from several milli-torr to approximately 40 torr for both propellants, and the stagnation temperature was about 295 K. The numerical modeling was performed with the DSMC method for stagnation pressures from 0.01 torr to 7.6 torr. The experiments were carried out for a single and dual orifice configurations; the computational studies also included four-orifice and an infinite array cases.

Both experimental and numerical results showed that for a dual orifice configuration there is no visible effect of jet interactions on orifice performance when the distance between the centers is one and a half or more orifice diameters. There was also a good agreement observed between the numerical and experimental data both for the mass flow and thrust.

Computations showed that there is a significant gas backflow observed for the four-orifice and array configurations. The force on the surface produced by the backflow amounts to over 16% of the orifice thrust force, with the specific impulse increasing over 20% compared to the single orifice.

Future work is planned in the following directions. First, the numerical studies will be performed for an array of orifices for different wall thickness and pressure values with the goal to determine the minimum pressure where the surface force is significant and still measurable. Then, experimental studies will be performed for this pressure in order to examine the surface force. Finally, the assessment of surface heat flux and its possible adverse effects on critical spacecraft surfaces will be performed for multiple orifice jets.

6 Acknowledgment

This work was supported by the Air Force Office of Scientific Research and the Propulsion Directorate of the Air Force Research Laboratory (Edwards AFB, CA). The authors also wish to acknowledge the help of Mr. Taylor Lilly with the experimental part of this work.

References

[1] Lewis, D., Janson, S., Cohen, R., Antonsson, E., "Digital Micropropulsion," *Sensors and Actuators,* Vol. 80, No. 2, 2000, pp. 143-154.

[2] Ketsdever, A., Green, A., Muntz, E.P., Vargo, S., "Fabrication and Testing of the Free Molecule Micro-Resistojet: Initial Results," *AIAA Paper 2000-3672*, Joint Propulsion Conference, 2000.

[3] Jamison, A., Ketsdever, A., Muntz, E.P., "Gas Dynamic Calibration of a Nano-Newton Thrust Stand," *Review of Scientific Instruments,* Vol. 73, No. 10, 2002, pp. 3629-3637.

[4] Ketsdever, A., "Facility Effects on Performance Measurements of Micropropulsion Systems Which Utilize Gas Expansion," *Journal of Propulsion and Power,* Vol. 18, No. 4, 2002, pp. 797-804.

[5] Selden, N., Ketsdever, A., "Comparison of Force Balance Calibration Techniques for the nano-Newton Range," *Review of Scientific Instruments,* Vol. 74, No. 12, 2003, pp. 5249-5254.

[6] Ivanov, M.S., Markelov, G.N., Gimelshein, S.F. "Statistical simulation of reactive rarefied flows: numerical approach and applications," *AIAA Paper 98-2669, June 1998*

[7] Ivanov, M.S., Rogasinsky, S.V., "Theoretical analysis of traditional and modern schemes of the DSMC method," *Proc. XVII Int. Symp. on Rarefied Gas Dynamics,* Aachen, Germany, 1991, pp.629-642.

[8] Bird, G.A., "Monte-Carlo simulation in an engineering context," *Rarefied Gas Dynamics,* edited by S. Fisher, Vol. 74, Progress in Astronautics and Aeronautics, 1981, pp. 239-255.

[9] Ketsdever, A.D., Green, A. and Muntz, E.P., "Momentum flux measurements from underexpanded orifices: application for micropropulsion systems," *AIAA Paper 2001-0502,* Jan. 2001.

Table 1: Impact of distance between orifices.

P_0,	Axisym		3D, $S = 0$		3D, $S = 2$ mm		3D, $S = 4$ mm	
torr	Mass Flow, kg/sec	Thrust, N	Mass Flow, kg/sec	Thrust, N	Mass Flow, kg/sec	Thrust, N	Mass Flow, kg/sec	Thrust, N
0.01	1.39e-9	5.29e-7	1.36e-9	5.20e-7	1.37e-9	5.22e-7	1.37e-9	5.22e-7
0.05	7.41e-9	2.90e-6			7.17e-9	2.82e-6		
0.1	1.52e-8	6.18e-6			1.50e-8	6.08e-6		
0.5	9.23e-8	4.28e-5			9.01e-8	4.18e-5	8.90e-8	4.13e-5
1.0	1.95e-7	9.57e-5			1.88e-7	9.29e-5		
4.0	8.45e-7	4.50e-4	8.14e-7	4.40e-4	8.12e-7	4.38e-4	8.21e-7	4.39e-4

Table 2: Performance characteristics for different configurations.

	$\dot{m}$, 10^{-6} kg/s	F_o, mN	F_s, mN	I_{sp}
AS	1.56	0.845	0.012	56.1
Single	1.53	0.834	0.012	56.4
Dual	1.5	0.835	0.022	58.3
Quadruple	1.49	0.823	0.042	59.2
Array	1.53	0.86	0.164	68.6

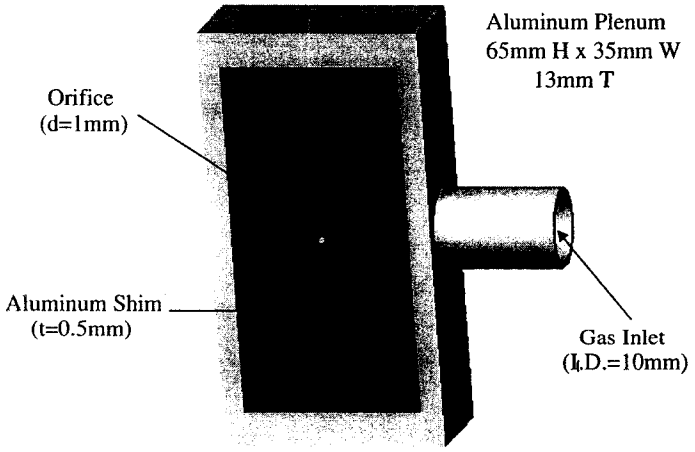

Figure 1: Schematic of single orifice mounted to the plenum.

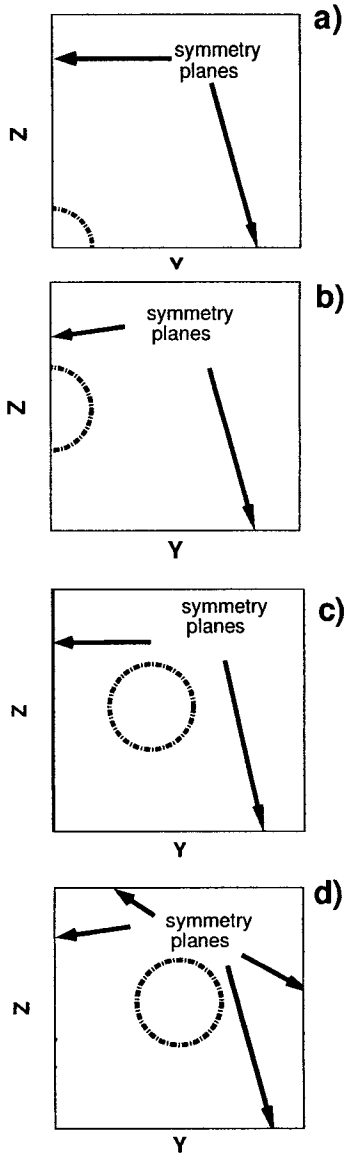

Figure 2: Schematic of the computational domain in YZ plane.

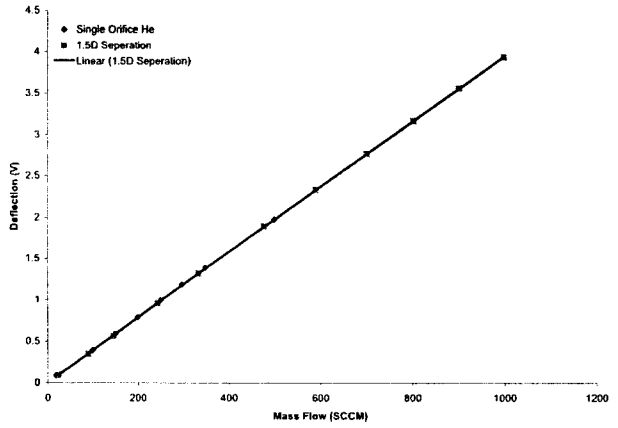

Figure 3: Force balance deflection versus helium mass flow for a single orifice and a dual orifice configuration with a 1.5 mm separation distance (center-to-center). Note: The dual orifice deflection has been divided by two for this comparison.

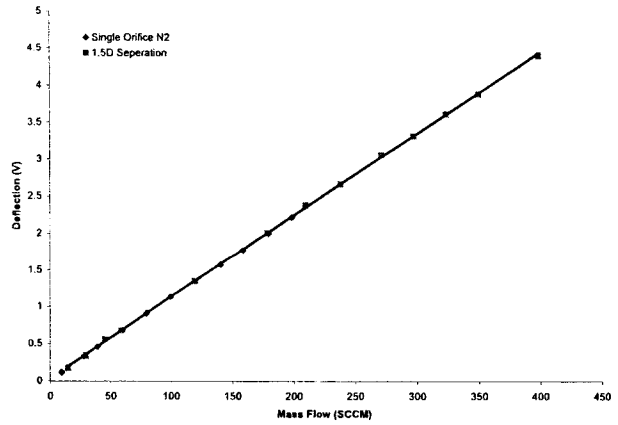

Figure 4: Force balance deflection versus nitrogen mass flow for a single orifice and a dual orifice configuration with a 1.5 mm separation distance (center-to-center). Note: The dual orifice deflection has been divided by two for this comparison.

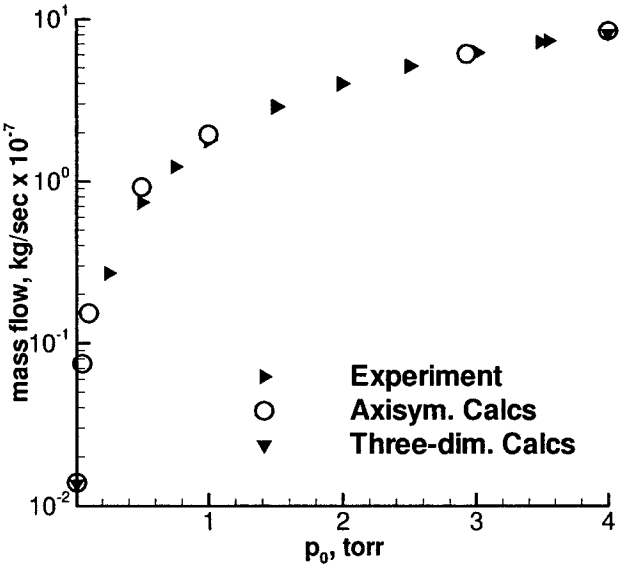

Figure 5: Mass flow for a single orifice: comparison with experimental data

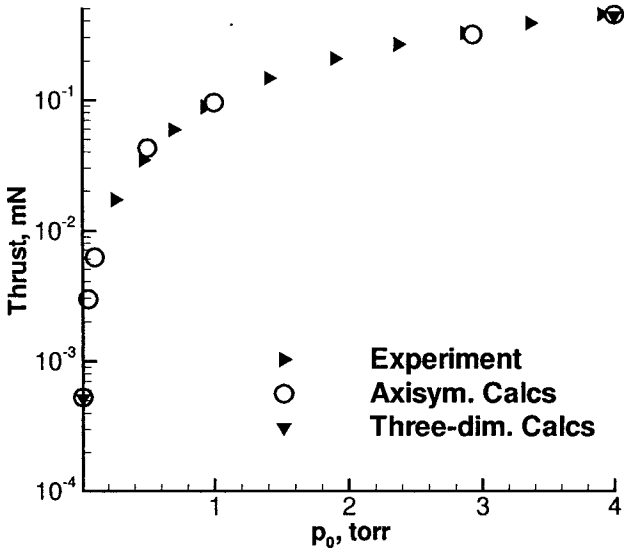

Figure 6: Thrust for a single orifice: comparison with experimental data

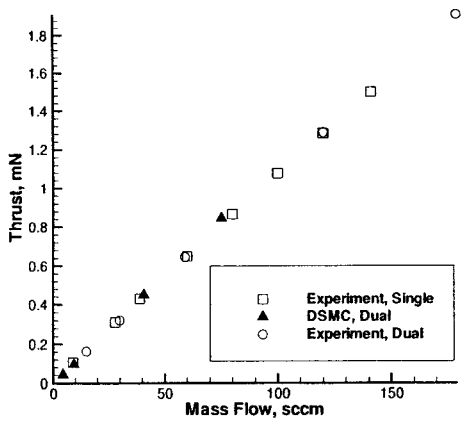

Figure 7: Comparison of experimental and numerical results for dual orifice case: thrust versus mass flow.

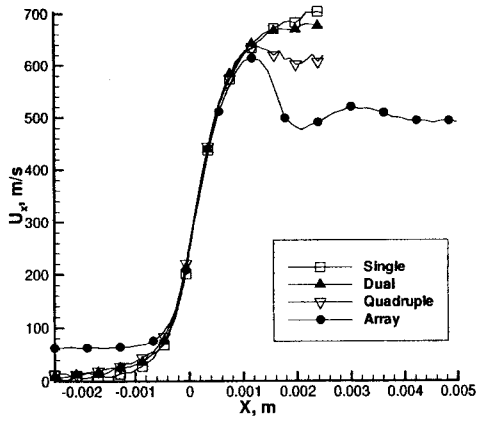

Figure 9: Velocity along X-axis.

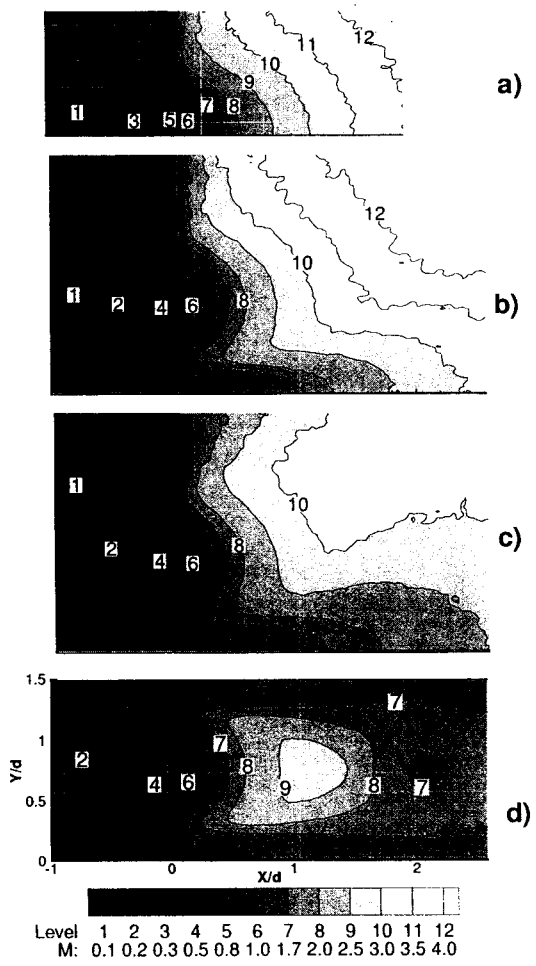

Figure 8: Mach number contours in XY plane. Nitrogen, $P_0 = 7.6$ torr. a) single orifice, b) dual orifice, c) quadruple orifice, d) orifice array.

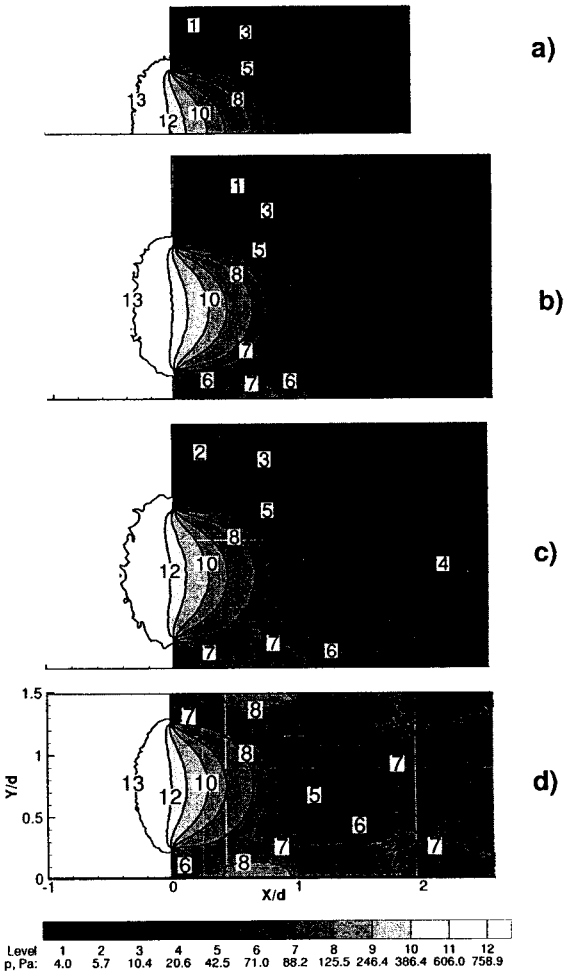

Figure 10: Pressure (Pa) contours in XY plane. Nitrogen, $P_0 = 7.6$ torr. a) single orifice, b) dual orifice, c) quadruple orifice, d) orifice array.

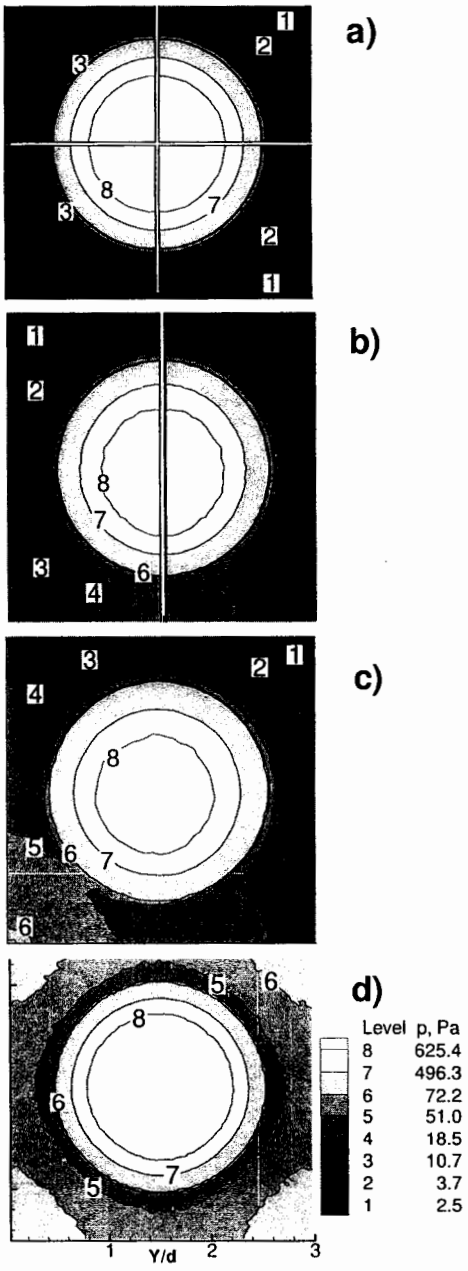

Figure 11: Pressure (Pa) contours in YZ plane near the surface. Nitrogen, $P_0 = 7.6$ torr. a) single orifice, b) dual orifice, c) quadruple orifice, d) orifice array.

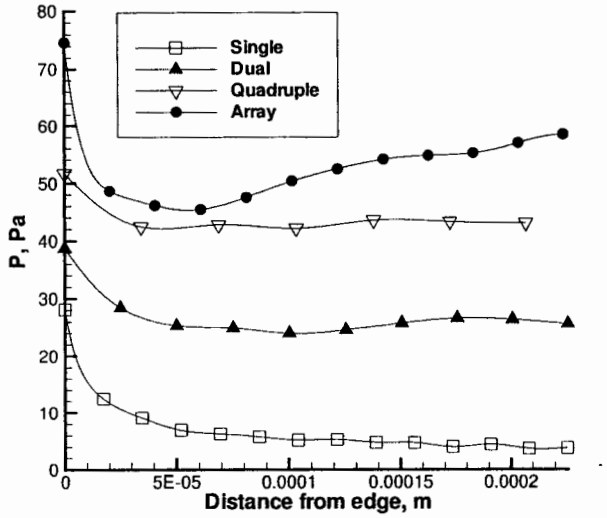

Figure 12: Pressure distribution near the surface for different configurations.